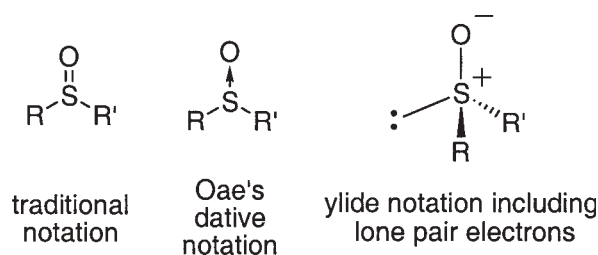


Photochemically Induced Stereomutation of Sulfoxides

William S. Jenks, Iowa State University

Introduction

The oxides of sulfur and phosphorus are treated with typographical disrespect. Finding a general chemistry textbook that has fewer than six bonds drawn to sulfur in sulfuric acid (H_2SO_4) is likely to be an impossible task. Likewise, nearly every phosphodiester drawn (e.g., in DNA structures) contains a $\text{P}=\text{O}$ double bond, for a total of five bonds to phosphorus. An irony is that true hypervalent hexavalent sulfur and pentavalent phosphorus are known, SF_6 and PCl_5 , for example. However, phosphine oxides, sulfoxides, sulfones, and related functional groups are not among the truly hypervalent.



Scheme 1

This is hardly a new issue. The bonding of the sulfate ion is discussed in Lewis's original paper that introduced the "dot structure."¹ Price and Oae's classic 1962 book *Sulfur Bonding* discusses the point at some length.² Based on experimental evidence available at the time, they conclude that a "semi-polar bond," i.e., a sigma bond plus an ionic bond, is the best representation for sulfoxides and sulfones. They represent this with the arrow notation of a dative bond, while still others (including ourselves, at least recently) use the ylide notation one would use for an amine oxide. (Scheme 1) This notation was criticized by Pauling³ in favor of resonance forms that had up to eight bonds to sulfur. The most recent Atoms-in-Molecules analysis of the sulfoxide bond⁴ sees it essentially as a single bond that is strengthened and shortened by electrostatic attraction. Localized molecular orbital views of the oxygen lone pairs show some distortion back towards the sulfur, consistent with this picture.

All of this is by way of emphasizing that the central atom in sulfoxides, sulfones, phosphine oxides, and related functional groups is approximately tetrahedral. With sulfoxides and sulfinyl functional groups in general, this implies that the sulfur is a stereogenic center, as long as the two other substituents are different. For simple sulfoxides, the barrier to racemization is of the order of 40 kcal/mol.⁵ Additionally, preparation of single enantiomers of a variety of sulfoxides is reasonably straightforward.⁶⁻⁸ These features, along with the directing ability of the polar SO bond have made sulfoxides attractive as chiral auxiliaries in organic synthesis.⁹⁻¹⁴

The configurational integrity of the sulfoxide has also generated interest in the various conditions under which it may undergo stereomutation. First noted by Krafft and Lyons over 100 years ago,¹⁵ the mechanisms of racemization of sulfoxides was first well reviewed by Mislow in 1967.¹⁶ Racemization is understood to occur by simple inversion of the sulfur center unless there are special structural features. Thiophene-based sulfoxides, for instance, have inversion barriers much lower than usual¹⁷ because the planar transition state has an aromatic stabilization not available to the starting material. Benzyl sulfoxides appear to racemize by a reversible homolysis of the C-S bond,¹⁸

Continued on page 3

From the Executive Director

D. C. Neckers, Executive Director, Center for Photochemical Sciences, Bowling Green State University

Lux Aeterna, Light Eternal

The events unfolding on September 11, 2001, have shaken the United States and much of the world to its core. We face uncertainty about our personal safety and the safety of our institutions that previous generations lived with, but we have never known.

The imagery of light appears frequently throughout music and the mass:

“Et lux perpetua luceat eis.”
“Let light perpetually shine upon them.”

For the victims on September 11 and their families.

For those in any other way effected by the events of September 11, physically or psychologically.

For those who were close to the events in the greater New York and Washington Metropolitan districts.

For the leaders of the world in this time of crisis.

For the leaders at the local level—university presidents, faculty leaders, staff leaders, and student leaders.

For our moral leadership—our clergy and philosophers.

For those who report the events to us—our reporters and writers.

For all our students and faculty but particularly for the students and faculty in American universities who came here from other nations.

For our enemies—whoever they are and wherever they might be.

And most of all let the light shine on each and every one of us so we'll know what to do next, how to react, and how to push on.

This is my wish for all of us in the days that lie ahead.

“Et lux perpetua luceat eis.”

In This Issue

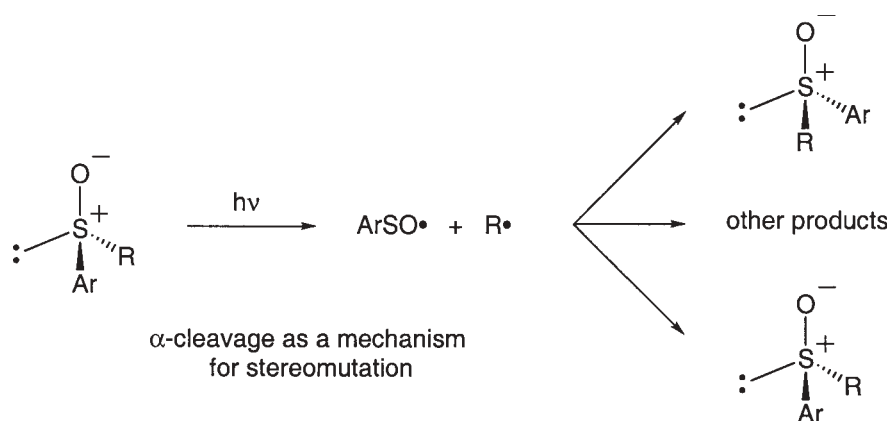
Photochemically Induced Stereomutation of Sulfoxides	1
From the Executive Director	2
Effects of Fluoro-Substituents on Excited State Properties of Conjugated Polyenes (Fluorinated Retinoids).....	8
Multiphoton Microscopy and Its Applications in the Biomedical Sciences	13

Continued from page 1

whereas allyl sulfoxides racemize by their reversible conversion to allyl sulfenic esters (RSOR').¹⁹ To the best of our knowledge, the edge inversion mechanism, in which the sulfoxide would fall in a T-shaped transition state (square planar including the lone pair), is not known for sulfoxides, though it has been invoked for the stereomutation of some phosphorus compounds.²⁰ Stereomutation of sulfoxides can also be induced by a variety of chemical agents, such as strong acids, acetic anhydride, N₂O₄, and butoxide,¹⁶ but we will restrict this discussion to unimolecular chemistry.

Photochemistry

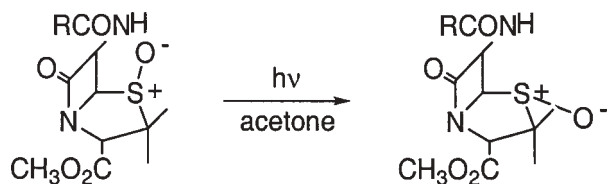
Stereomutation is also an important part of the photochemistry of sulfoxides. Our own work has been limited mainly to alkyl aryl sulfoxides and diaryl sulfoxides, but previous workers have looked at dialkyl cases and have also observed stereomutation at the sulfur center. It is our observation that the unimolecular photochemistry of most aromatic sulfoxides consists largely of α -cleavage reactions and epimerization of the sulfinyl group.^{21, 22} The proclivity for α -cleavage, as measured by chemical quantum yields and quantum yields of free sulfinyl radicals,²³ varies with the alkyl substituent in predictable fashion. Since the sulfinyl radical is not stereogenic, and recombination of the sulfinyl and carbon-centered radicals may occur with either orientation at sulfur, α -cleavage represents a clear mechanism by which racemization may occur. (Scheme 2) In the rest of this article, we examine the evidence accumulated over the years for this mechanism, and in particular whether it accounts for *all* of the photochemical racemization of sulfoxides. We conclude that the weight of the evidence is now that there is an additional, non-homolytic mechanism that is involved.



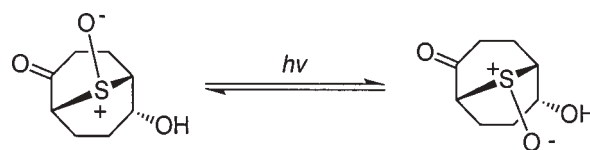
Scheme 2

The earliest work on photochemical stereomutation of sulfoxides was done in a collaboration between the groups of George Hammond and Kurt Mislow. They reported conditions under which naphthyl tolyl sulfoxide and other alkyl tolyl sulfoxides could be partially or fully racemized in competition with uncharacterized decomposition reactions.²⁴ Their interest quickly turned to the phenomenon of naphthalene-sensitized racemization of alkyl tolyl sulfoxides, which was particularly interesting in that energy transfer from naphthalene to a tolyl sulfoxide is not energetically plausible in either the singlet or triplet manifold. This sensitized reaction became one of Hammond's cases of reactive exciplexes,²⁵ though the details of how the reaction might proceed were never elucidated. The concept of sensitized racemization leads immediately to the use of an optically pure chiral sensitizer to resolve sulfoxides, an exercise carried out by the Kagan group a few years later, albeit with only modest success.²⁶

Several cases of photochemical stereomutation of dialkyl sulfoxides were also reported during this period. Important chemistry allowing the preparation of cephalosporins from penicillins involves the intermediacy of the penicillin sulfoxides. Oxidation of several penicillin derivatives by a variety of chemical methods produced only the (*S*) configuration of the sulfoxide and standard chemical means of inverting that center in order to study the chemistry of the (*R*) isomer failed, and the first synthesis of an (*R*) penicillin sulfoxide was accomplished by Archer by photolysis of the (*S*) isomer in acetone. The reaction yielded a single product, but a yield was not reported.²⁷ Similar chemistry was elaborated by Stry in more complex systems.²⁸ (Scheme 3)



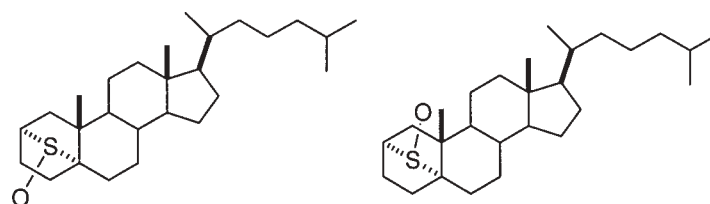
Scheme 3



Scheme 4

Other papers discussed mechanism as part of their reports. A number of aliphatic and cyclic β -ketosulfoxides were shown to undergo stereomutation of the sulfinyl group.²⁹ The authors proposed that an internal energy transfer occurred from the carbonyl to the sulfinyl group, but in hindsight it seems more likely that the reaction is essentially a case of β -cleavage of the carbonyl group that produces the same radical pair or biradical that would be formed by a classic sulfoxide α -cleavage reaction. (Scheme 4)

Kishi took advantage of diastereomeric interactions to achieve nearly the equilibrium mixture of the two sulfoxides deriving from 5 α -cholestane-2 α -5-episulfide, starting with a clean sample of either isomer.³⁰ The ratios that could be obtained, however, were not identical, and Kishi argued that this suggested the mechanism was not simple pyramidal inversion of sulfur. (Scheme 5)



92	:	3	equilibrium
90	:	10	hv, starting with major isomer
77	:	23	hv, starting with minor isomer

Scheme 5

Mechanistic Considerations

The above chemistry, carried out in the late 1960s and early 1970s, was speculative in its mechanistic interpretation. None of these results required any explanation beyond a reversible α -cleavage event, though beginning even as early as Hammond's work there was suggestion of a direct inversion mechanism. The underlying assumption of this suggestion is that, in analogy to the cis-trans isomerization of olefins, there is a rearrangement of geometry in an excited state—presumably to a planar sulfur center—that allows relaxation to either the *R* or *S* configuration when the molecule finds a way back down to the ground electronic state, as illustrated in Figure 1.

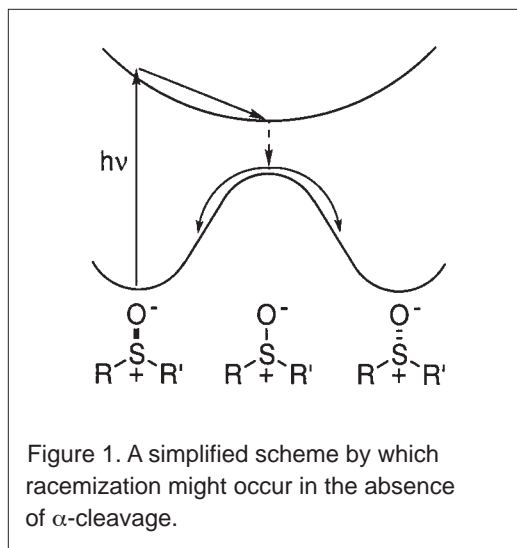
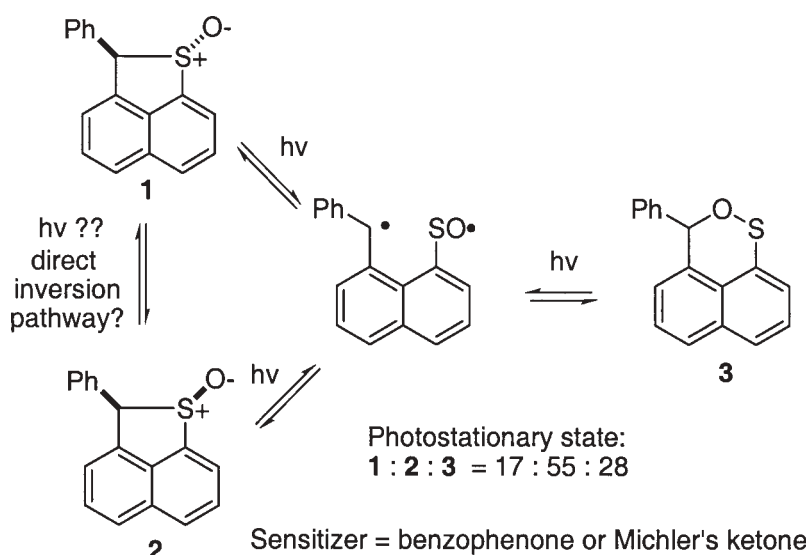


Figure 1. A simplified scheme by which racemization might occur in the absence of α -cleavage.

This view was first strongly advocated by Schultz and Schlessinger, who studied racemic samples of a cyclic naphthyl-benzyl sulfoxide. (Scheme 6) They were able to achieve a triplet sensitized photostationary state that included both sulfoxide isomers **1** and **2** and the sultene **3**. High quantum yields for the interconversions were used as justification for the inversion mechanism, though they acknowledged that α -cleavage was involved in the formation of the sultene. Again, with hindsight, it is difficult to see why high quantum yields demand anything but efficient α -cleavage. In fact, similarly high quantum yields are observed for decomposition of phenyl benzyl sulfoxides, in chemistry that was clearly dominated by α -cleavage.²¹

Kropp's 1991 data on the photolysis of tolyl 2-norbornyl sulfoxides might also be interpreted as circumstantial evidence for a non-cleavage pathway. Photolysis of **4** led to much faster epimerization of the sulfur



Scheme 6

ond flash photolysis follows a very similar trend.²³ Thus, unless it is proffered that the primary systems undergo α -cleavage at the same or higher total efficiency as benzyl systems but suffer geminate recombination with the sulfinyl radical particularly efficiently, it must be concluded that primary systems simply undergo α -cleavage with lower efficiency. Such an interpretation is made particularly plausible by the observation that the major chemical product in most cases is the sulfenic ester Ph-S-O-R. There seems little reason to suggest that primary alkyl groups would form the sulfoxide to the near exclusion of the sulfenic ester when reacting with sulfinyl radicals.

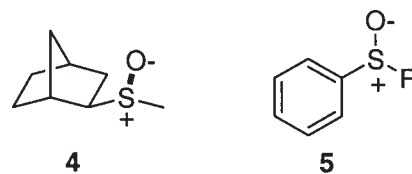
Within this context, the case of optically pure methyl tolyl sulfoxide is intriguing. In isopropanol, the optical rotation of a sample is lost with a quantum yield of 0.90, while the sulfoxide disappears with a quantum yield of only 0.036. Since products do not contribute to the optical rotation, a sulfur inversion quantum yield of 0.43 is obtained. If it is assumed that the inversion event produces either epimer with equal likelihood (as would, for example, α -cleavage) then the quantum yield for the racemization event is 0.86 in addition to any events that lead to new chemical products. If there is not pathological recombination selectivity for the sulfoxide over the sulfenic ester, then this represents good circumstantial evidence for a non α -cleavage racemization mechanism.

Related experiments from two research groups have recently appeared in which the phenyl or tolyl group is replaced by a more emissive chromophore, such as pyrene, anthracene, etc.³²⁻³⁴ Both groups showed that reasonable inversion quantum yields are accompanied by fluorescence quantum yields that are much lower than for the unsubstituted arenes. For example, Tsurutani finds Φ_f of 0.002 for phenanthryl *p*-tolyl sulfoxide in methanol. Similarly, both groups find low quantum yields for degradation of the materials, approximately 0.03 for phenanthryl *p*-tolyl sulfoxide in methanol. The inversion quantum yield is 0.3. In a series of aryl methyl compounds, Lee³⁴ showed that the suppression of fluorescence was unique for sulfoxides among sulfides, sulfoxides and sulfones, ruling out a sulfur heavy-atom effect. Furthermore, sensitization and triplet quenching experiments showed that the inversion event occurs from the singlet manifold. Again, the evidence is circumstantial, but the most straightforward conclusion is that sulfoxide inversion is the result of a non-radiative relaxation pathway of the singlets of these aromatic chromophores.

If the mechanistic scheme implied by Figure 1 is to be taken seriously, some evidence of a relaxation of the excited state geometry to a planar conformation would be extremely important. A computational chemistry investigation on the ground and excited state structures of dimethyl sulfoxide (DMSO) has recently been completed.³⁵ DMSO is obviously not chiral, but its inversion is a model for any dialkyl sulfoxide and the increased symmetry makes the

center than the 2-norbornyl position.³¹ However, it must be remembered in this case that there is necessarily a diastereoselectivity, and the apparent lack of carbon epimerization may simply reflect the selectivity of the recombination step.

Photolysis of a series of simple phenyl alkyl and tolyl alkyl sulfoxides presents better indirect evidence for a non-radical pathway. Photolysis of sulfoxides of the type 5 (Scheme 7) produces products that are, aside from minor amounts of deoxygenation, attributable to singlet α -cleavage chemistry.^{21,22} Quantum yields for total disappearance of starting material follow a reasonable "stability of R•" profile, though quantum yields are very similar for R = primary and R = phenyl. On a shorter timescale, the quantum yield of formation of PhSO• observable by nanosec-



Scheme 7

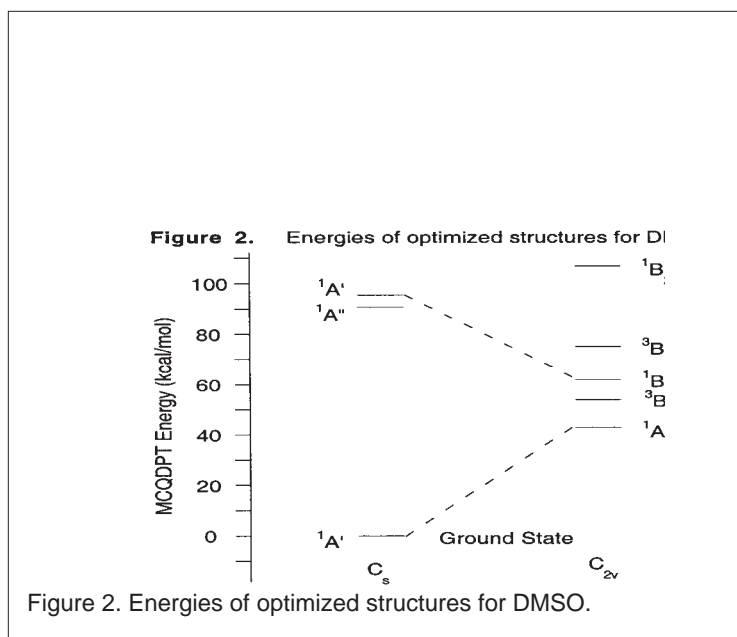
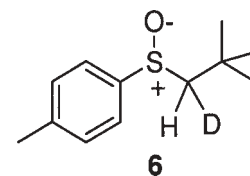


Figure 2. Energies of optimized structures for DMSO.

calculations more straightforward than those for a chiral sulfoxide would be. In this work, CASSCF calculations³⁶ were completed on ground and excited states, with multireference MP2 corrections done on the energies. On the ground state, an inversion transition state with a C_{2v} symmetry is found 41.5 kcal/mol above the relaxed geometry. The energies of the low lying $1A'$ and $1A''$ states at the ground state geometries were within a very few kcal/mol of the observed λ_{\max} values in the gas phase UV absorption spectrum of DMSO. Relaxed geometries (i.e., stationary points) were obtained on the excited state surfaces in both C_s and C_{2v} symmetry. As shown in Figure 2, there is a strict correlation between the lowest excited $1A'$ state and a planar $1B_1$ geometry, with the $1B_1$ state being considerably downhill from either the vertical excited state energy or any C_s stationary point that could be found. Moreover, at the geometry of the $1B_1$ stationary point, the ground and excited state potentials are separated by fewer than 10

kcal/mol, so funneling of molecules from the excited state down to a planar (and thus stereochemically indifferent) geometry should be very efficient. These calculations make the case clearly enough for dialkyl sulfoxides that a non-radiative, non-cleavage pathway for sulfoxide inversion is plausible. Extension of this work to the more difficult alkyl aryl case is ongoing.

However, recent experimental results on a new alkyl aryl sulfoxide provide very strong evidence for the existence of the non-radical path.³⁷ Preparation of a single diastereomer of sulfoxide **6** allows analysis of the mixture of diastereomers produced on photolysis to low conversion. Because there is no diastereomeric preference for the recombination product **6** in that the second stereogenic center is a CHD methylene, α -cleavage chemistry will lead to equal production of all three of the other diastereomers. However, inversion of the sulfur without cleavage results in formation of only a single diastereomer, the one in which only the sulfur center has been epimerized. The experimental result is that, on direct photolysis, there is a strong preference for the predicted diastereomer in which only the sulfur is inverted. It can thus be concluded that the non-cleavage photochemical stereomutation pathway suggested decades ago with support only from chemical intuition is indeed a real phenomenon.



Scheme 8

Summary

Aromatic sulfoxides are subject to photochemical stereomutation in relatively high quantum yield. Though this fact has been known for some time, discussions of the mechanism were for the most part speculative. It is now well established that at least a fraction of photochemical stereomutation occurs as a result of recombination of radicals borne of α -cleavage chemistry. In addition, however, evidence from quantum yields, computational chemistry, and experiments with molecules containing two adjacent stereogenic centers point very strongly to a competing non-homolytic mechanism. In light of computational chemistry results with DMSO, it is proposed that the additional epimerization derives from geometrical relaxation in the excited state that results in a non-stereogenic sulfur center. Upon returning to the ground electronic state, relaxation to the *R* and *S* configurations is competitive.

References

1. Lewis, G. N. *J. Am. Chem. Soc.* **1916**, *38*, 762-785.
2. Price, C. C.; Oae, S. *Sulfur Bonding*; Ronald Press: New York, 1962.
3. Pauling, L. *The Nature of the Chemical Bond and the Structure of Molecules and Crystals*, 3rd ed.; Cornell University Press: Ithaca, NY, 1960.

4. Dobado, J. A.; Martinez-Garcia, H.; Molina, J. M.; Sundberg, M. R. *J. Am. Chem. Soc.* **1999**, *121*, 3156-3164.
5. Rayner, D. R.; Gordon, A. J.; Mislow, K. *J. Am. Chem. Soc.* **1968**, *90*, 4854-4860.
6. Andersen, K. K. In *The Chemistry of Sufoxides and Sulfoxes*; Patai, S., Rappoport, Z., Stirling, C. J. M., Eds.; John Wiley & Sons Ltd.: New York, 1988, pp 55-94.
7. Allin, S. M. *Organosulfur Chem.* **1998**, *2*, 41-61.
8. Skarzewski, J.; Ostrycharz, E. *Wiad. Chem.* **2000**, *54*, 725-758.
9. Carreño, M. C. *Chem. Rev.* **1995**, *95*, 1717-1760.
10. Carretero, J. C.; Arrayas, R. G.; Buezo, N. D.; Garrido, J. L.; Alonso, I.; Adrio, J. *Phosphorus, Sulfur Silicon Relat. Elem.* **1999**, *153-154*, 259-273.
11. Metzner, P.; Alayrac, C.; Julienne, K.; Nowaczyk, S. *Actual. Chim.* **2000**, 54-59.
12. Bravo, P.; Zanda, M. *Enantiocontrolled Synth. Fluoro-Org. Compd.* **1999**, 107-160.
13. Matsuyama, H. *Sulfur Rep.* **1999**, *22*, 85-121.
14. Allin, S. M.; Shuttleworth, S. J.; Bulman Page, P. C. *Organosulfur Chem.* **1998**, *2*, 97-155.
15. Krafft, F.; Lyons, R. E. *Chem. Ber.* **1896**, *29*, 435-436.
16. Mislow, K. *Rec. Chem. Prog.* **1967**, *28*, 216-240.
17. Mock, W. L. *J. Am. Chem. Soc.* **1970**, *92*, 7610-7612.
18. Miller, E. G.; Rayner, D. R.; Thomas, H. T.; Mislow, K. *J. Am. Chem. Soc.* **1968**, *90*, 4861-4868.
19. Bickart, P.; Carson, F. W.; Jacobus, J.; Miller, E. G.; Mislow, K. *J. Am. Chem. Soc.* **1968**, *90*, 4869-4876.
20. Arduengo, A. J., III; Stewart, C. A. *Chem. Rev. (Washington, D. C.)* **1994**, *94*, 1215-1237.
21. Guo, Y.; Jenks, W. S. *J. Org. Chem.* **1995**, *60*, 5480-5486.
22. Guo, Y.; Jenks, W. S. *J. Org. Chem.* **1997**, *62*, 857-864.
23. Darmanyan, A. P.; Gregory, D. D.; Guo, Y.; Jenks, W. S. *J. Phys. Chem. A* **1997**, *101*, 6855-6863.
24. Mislow, K.; Axelrod, M.; Rayner, D. R.; Gottardt, H.; Coyne, L. M.; Hammond, G. S. *J. Am. Chem. Soc.* **1965**, *87*, 4958-4959.
25. Cooke, R. S.; Hammond, G. S. *J. Am. Chem. Soc.* **1970**, *92*, 2739-2745.
26. Balavoine, G.; Jugé, S.; Kagan, H. B. *Tetrahedron Lett.* **1973**, 4159-4162.
27. Archer, R. A.; De Marck, P. V. *J. Am. Chem. Soc.* **1969**, *91*, 1530-1532.
28. Spry, D. O. *J. Am. Chem. Soc.* **1970**, *92*, 5006-5008.
29. Ganter, C.; Moser, J.-F. *Helv. Chim. Acta.* **1971**, *54*, 2228-2251.
30. Kishi, M.; Komeno, T. *Tetrahedron Lett.* **1971**, *28*, 2641-2644.
31. Kropp, P. J.; Fryxell, G. E.; Tubergen, M. W.; Hager, M. W.; Harris Jr., G. D.; McDermott Jr., T. P.; Tornero-Velez, R. *J. Am. Chem. Soc.* **1991**, *113*, 7300-7310.
32. Tsurutani, Y.; Yamashita, T.; Horie, K. *Polymer Journal* **1998**, *30*, 11-16.
33. Tsurutani, Y.; Machida, S.; Horie, K.; Kawashima, Y.; Nakano, H.; Hirao, K. *J. Photochem. Photobiol., A* **1999**, *122*, 161-168.
34. Lee, W.; Jenks, W. S. *J. Org. Chem.* **2001**, *66*, 474-480.
35. Cabbage, J. W.; Jenks, W. S. *J. Phys. Chem.* **2001**, in press.
36. The orbital active space was full valence, excepting the CH bonds. The basis set was 6-311+G(3df).
37. Vos, B. W.; Jenks, W. S. *manuscript in preparation* **2001**.

About the Author

William Jenks received his Ph.D. with Nick Turro at Columbia in 1991, where he studied spin polarization transfer phenomena in time-resolved EPR. He moved downstairs two floors to work as a postdoctoral associate with Ronald Breslow while his wife Cynthia finished her Ph.D, also in chemistry. The Drs. Jenks moved to Iowa State in 1992. William's group has interests in organosulfur chemistry, photocatalytic degradation, and the application of computational chemistry to physical organic chemistry. He can be reached at 515-294-4711 or wsjenks@iastate.edu.

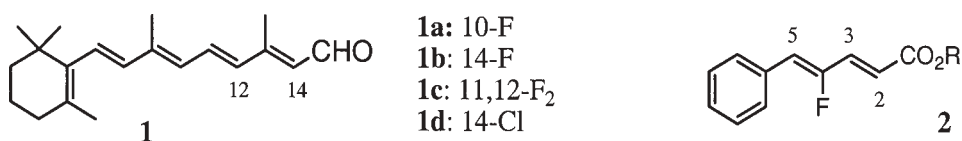
Effects of Fluoro-Substituents on Excited State Properties of Conjugated Polyenes (Fluorinated Retinoids)

Leticia U. Colmenares, Alfred E. Asato and Robert S. H. Liu
Department of Chemistry, University of Hawaii

In recent decades we have prepared a large number of retinal (**1**) analogs¹ with fluorine labels on the ring as well as on the polyene side chain. Subsequently, many fluorinated rhodopsin and bacteriorhodopsin (bR) analogs were prepared, which provided a rich collection of F NMR data for examining protein-substrate interactions. Throughout these studies, we observed, on occasion, the specific role of the F-substituent imparting unique photochemical or absorption properties on the labelled polyenes. Some of these observations have since been amplified in designed fluorinated substrates for photochemical studies, preparation of long-wavelength absorbing pigments and unusual photophysical and circular dichroism (CD) characteristics. In this paper, we summarize the effects of F-substituents on excited state properties of polyenes, especially the retinoids.

Regioselective Photoisomerization

F-substituents exert a definite regioselective effect on photoisomerization of retinals. For example, in the case of photoisomerization of all-*trans*-retinal (**1**) in a non-polar hexane, the regioselective formation of the 13-*cis* and the 9-*cis* isomers (in a ratio of 4.0 to 1) was changed to new ratios of 3.1:1 and 2.3:1 for 10F-retinal and 14F-retinal, respectively.² More spectacular regiospecific perturbation of the F-substituents on photoisomerization was shown in the following two examples. For the 4-fluorodienester **2**, direct irradiation was found to lead to regiospecific photoisomerization at the 4,5-bond rather than the non-selective result for the unsubstituted parent diene ester.³ The perturbation was attributed to selective formation of the zwitterionic intermediate stabilized by the F-substituent.



The second example of regiospecific isomerization was observed in fluorinated rhodopsin analogs. Bathorhodopsin, the all-*trans* primary photoproduct of rhodopsin, is known to undergo secondary photoisomerization reversibly to the 11-*cis* rhodopsin and to the isomeric 9-*cis* pigment in an approximate ratio of 3:1.⁴ However, in the case of 10-fluororhodopsin, the corresponding bathorhodopsin was found to isomerize regiospecifically to the 11-*cis* with no detectable amount of the 9-*cis* isomer. At the same time the 9-*cis*-10-F-rhodopsin pigment was found to be photostable at liquid nitrogen temperature.⁵ The loss of reactivity of photoisomerization was shown to be regiospecific at the 9,10-bond because bathorhodopsins with the F-label located on other positions of the polyene chain isomerized in the same manner as the parent system. Regiospecific isomerization at the 11,12-position is due to supramolecular control by the binding pocket with isomerization at the 9,10-bond hindered by specific protein perturbation either in the form of H,F hydrogen bonding attractive interaction with a nearby acidic protein residue⁶ or repulsive interactions of F with a nearby electron rich residue.⁵

The Use of Three-Bond Coupling Constants in Following Photoisomerization of a Visual Pigment Analog

For some time, the potential application of vicinal coupling constants involving F-substituents was recognized.⁷ The three-bond H,H H,F or F,F coupling constants share the similar trend in that the respective values for the *cis* isomers (11-13, 5-20, 0-30 Hz) are smaller than the corresponding values of the *trans* (15-17, 25-35, >100 Hz).⁸ Since the linewidths of NMR signals of detergent solubilized globular proteins like rhodopsin are usually >200 Hz, it will be impossible to follow the *cis* to *trans* isomerization of visual pigments using H,H or H,F coupling constants. The

large difference between three-bond F,F coupling constants of the *trans* and *cis* isomers provides possibly a useful handle. Its application to photochemistry of rhodopsin became possible after successful synthesis of the key 11-*cis*-11,12-difluororetinol (**1a**).⁸

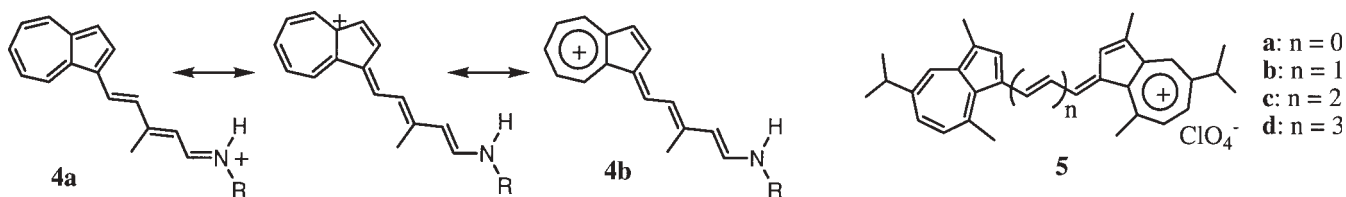
The resultant 11,12-difluororhodopsin showed absorption ($\epsilon_{\max} = 503.5$ nm) and photochemical properties similar to those of rhodopsin ($\epsilon_{\max} = 498$ nm).⁸ After irradiation of a detergent solubilized sample of the pigment analog at room temperature, the two broad singlets in the F NMR spectrum corresponding to the two vicinal F-labels were converted to two sets of higher field signals. The latter correspond to those of the free all-*trans*-11,12-difluororetinol (sharper) and the random Schiff bases of the retinal (broader). The F-12 signal of the free retinal was sufficiently well resolved, appearing as a clean doublet with a coupling constant of 104 Hz. The observation of the large coupling constant that is only consistent with formation of the *trans* isomer is perhaps an unnecessary confirmation of 11-*cis* to 11-*trans* isomerization of the retinyl chromophore in the primary photochemical process of the visual process.⁹ But importantly, it established for the first time the possible application of a simple organic technique for configurational assignment of isomers to a protein sample. The method is potentially useful for elucidation of the photochemical processes in any other photosensitive confined chromophores (e.g., photoactive yellow protein or other retinoid binding proteins).¹⁰

Perturbation of Absorption Maxima – Preparation of NIR Absorbing Pigments

During the course of preparing F-rhodopsin and F-bR analogs, we observed an interesting dependence of the pigment absorption maxima on the location of the vinyl F-substituent. Thus, within the set of analogs with the F-substituent on even-numbered carbon on the retinal side chain, the pigment was found to be red-shifted when the substituent was located close to the aldehyde end group and blue-shifted if located near the ring (530, 562, 566 and 583 nm for 8-F, 10-F, 12-F and 14-F bR's, respectively).¹¹ Since retinal is bound to opsin through a protonated Schiff base (PSB) linkage, we rationalized the red-shift to destabilization of the ground state PSB due to the proximity of the highly electron withdrawing substituent to the positively charged nitrogen.

These features have since been incorporated into the strategy of preparing red-shifted pigments including the near IR (NIR) absorbing bR pigments (up to 830 nm).¹² We found that F-substituent in the azulenic retinal analogs not only can enhance red-shift of the resultant bR analogs, but also lead to new cyanine-like (narrow absorption band) pigments.^{12,13} For example, the bR pigments derived from 4-methylazulenedialdehyde (**3a**),

6-methylazulenedialdehyde (**3b**), 6-*t*-butylazulenedialdehyde (**3c**) and 6-*t*-butylazulene-2'-fluorodialdehyde (**3d**) show progressive change of absorption from a broad band at 620 nm (**3a**) to a narrow band at 686 nm (**3d**). The latter narrow, red-shifted absorption bands are similar to those of the cyanine dyes, attributable to the involvement of the resonance stabilized tropylium ion (**4b**) in enhancing the formation of the fully delocalized PSB cation in addition to the initial iminium ion (**4a**). This interpretation was supported by comparison with the absorption spectra of the fully delocalized azulenic cyanine dyes (**5**).¹³



Close proximity of the strongly electron-withdrawing F-substituent to the positively charged nitrogen has a profound effect on the acidity of the nearby PSB. Sheves and coworkers showed that the 13-CF₃-substituent significantly alter the photobleaching characteristics of the bR analog.¹⁴

In a different application we showed that the π -donating characteristics of the F-substituent can be used to perturb the energy levels of the excited states of the azulene chromophore. The net result, from selective lowering of the S₁-state, was the preparation of a unique compound (1,3-difluoroazulene, **6**) with a larger S₂-S₁ energy gap than that of S₁-S₀. Its S₂-fluorescence yield (up to 0.2) and lifetime (~10 nsec) are the largest known for an upper singlet state.¹⁵

CD Characteristics of F-Rhodopsins

The retinyl chromophore in bovine rhodopsin is chiral as demonstrated by its prominent CD characteristics. The visible CD spectrum of 11-*cis*-rhodopsin in 2% CHAPS detergent showed two positive monophasic CD bands: 334 nm (β -band) and 493 nm (α -band) corresponding to the beta and alpha absorbance wavelength maxima (Figure 1). The intensity ratio for the β/α bands is 1.7. Its CD intensity ratio varies with the detergent used: 1.4 in 2% digitonin and 3.5 in octyl glucoside.¹⁶

Table 1. The CD (maximum wavelength, nm and $\Delta\epsilon$ values) and absorption data of 11-*cis*-rhodopsin and fluorinated analogs in 2% CHAPS.

Rhodopsins	β -CD, nm ($\Delta\epsilon$)	α -CD, nm ($\Delta\epsilon$)	Absorption λ_{\max} , nm
11c-parent	334 (17.0)	493 (9.9)	500
11c-8-F	340 (12.7)	442 (5.6)	463
11c-9-CF ₃	337 (12.2)	446 (5.2)	456
11c-10-F	336 (27.2)	496 (12.3)	499
11c-11-F*	332 (21.5)	Negligible	489
11c-12-F*	346 (13.0)	506 (2.4)	507
11c-13-F*	337 (24.2)	Negligible	502
11c-14-F	350 (8.6)	528 (5.3)	527
11c-11,12-F ₂ *	340 (19.7)	494 (-8.6)	504
11c-8,12-F ₂ *	346 (12.4)	484 (-3.4)	476

During the course of preparation of the F-rhodopsins, we have accumulated a large number of hitherto unpublished CD spectra of these pigment analogs. The UV and CD data for the 11-*cis* isomers are tabulated in Table 1. A majority of the F-rhodopsin analogs have β/α CD ellipticities similar to those of the parent rhodopsin. However, major deviations were observed in the following analogs: 11-*cis*-12-F, 11-*cis*-11-F, 11-*cis*-11,12-F₂, 11-*cis*-8,12-F₂, 11-*cis*-13-F and 9,11-*dicis*-12-F. For comparison, the spectra of some of the 11-*cis*-F-analogs are shown along with that of rhodopsin in Figure 1.

The distorted conformation of the 11-*cis* retinyl chromophore either due to internal steric crowding around the C12-C13 bond and the C6-C7 bond imparts chirality to the molecule, but no detectable CD spectra for solution samples. Only when protein bound, selective twists around the C12-C13 and C6-C7 bonds are induced giving rise to the α and β Cotton effects, respectively. It was estimated that the absolute twist at C12-C13 by exciton-coupling method is about -130 to -150 degrees.¹⁷

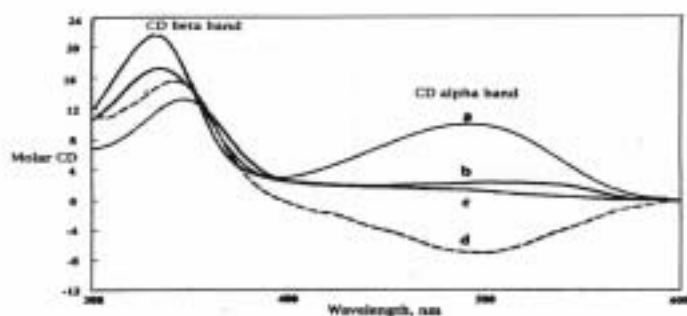
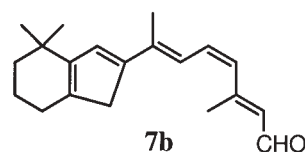
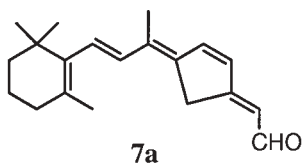
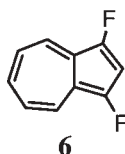


Figure 1. CD spectra of visual pigment analogs (a) 11-*cis*-rhodopsin (b) 11-*cis*-12-F (c) 11-*cis*-11-F (d) 11-*cis*-11,12-F₂-rhodopsin

The absence of said chromophoric twists in rhodopsin analogs, such as those reconstituted with ring-locked retinals actually resulted in weak Cotton effects. The 5-membered bridged 10C-13CH₃ analog (**7a**) gave negligible α -CD band and 5-membered bridged 8C-5CH₃ analog (**7b**) gave weak β -CD band.¹⁸ The weak α -bands in 11-*cis*-11-F and 12-F rhodopsin analogs (see Figure 1) however, cannot be rationalized by planarization about C12-C13. The biochemical characteristics of said analogs, such as rate of binding, pigment yield, stability, photobleaching property, UV absorption and UV opsin shifts are all similar with those of the parent rhodopsin indicating similar conformational structure. Moreover, molecular geometry optimization by semi-empirical AM1 calculations (HYPERCHEM) show that replacement of an H with F in the free chromophore



actually enhances the twist in the adjacent C-C single bond. For example, substitution of H with F in position 12 increases the C12-C13 twist. In the case of 13F analog however, the F replacement of the bigger methyl group reduces the C12-C13 torsional twist to -167 degrees vis-a-vis that of the parent 11-*cis*-retinal of -137 degrees. All others, including the 11,12-F₂ analog maintained similar C12-C13 dihedral angle to the parent, ranging from -131 to -142 degrees.

We suspect the intrinsic properties of the F-substituent on the helical polyene chromophore plays a significant role. In Brewster's rules for predicting magnitude of optical rotation, the F-substituent, with a small atomic refractivity, is the only one among the common substituents with a negative specific rotatory power.¹⁹ Compared to other substituents, F is known to cause sign reversal of the CD or ORD spectra of saturated ketones and steroid ketones.²⁰ However, in steroid ketones for example, this phenomenon only manifests itself in certain positions (i.e. axial α -position to keto group). Qualitatively, we see the same role played by the F-substituent on the helical 11-*cis*-retinyl chromophore. The decrease in α -CD band intensity is apparent when F is located nearest to the center of twisting (C12-C13), as in 11-F, and 12-F analogs. When more than one F is present, as in the 11,12-F₂ analog, the effect on the CD is additive, resulting in a negative α -CD band.

Quantitatively, at this time it is difficult to account for all finer details pertaining to the variation of the CD curves. We suspect not only the location of the F-substituent is important but so is its effect on the electron density of the polyene chromophore and any resultant changes, in electric transition dipole moment of the polyene chromophore. Model compounds involving simple F-substituted chiral chromophore that are helical, coupled with calculations, will be highly desirable for a better understanding of F-effect on CD.

In summary, in this article we have demonstrated that F-substituents serve more than NMR reporters. When properly placed, it may produce desirable perturbation on excited state properties of polyenes and presumably other chromophores.

Acknowledgment

The work was supported by grants from U.S. Public Health Services (DK-17806) and Army Research Office (DAAH04-96-1-0031). We acknowledge with thanks a helpful discussion with Professor Nakanishi on CD properties of F-rhodopsins.

References

1. Liu, R. S. H.; Asato, A. E. In *Chemistry and Biology of Synthetic Retinoids*; Dawson, M.; Okamura, W. H., Eds.; CRC Press, 1990; pp 51-75.
2. (a) Liu, R. S. H.; Asato, A. E. *Tetrahedron* **1984**, *40*, 1931. (b) Liu, R. S. H. In *CRC Handbook of Organic Photochemistry and Photobiology*; Horspool, W. M.; Song, P. S., Eds.; CRC Press, 1995; pp 165-172.
3. Muthuramu, K.; Liu, R. S. H. *J. Am. Chem. Soc.* **1987**, *109*, 6510.
4. Shichida, Y.; Yoshizawa, T. *Method Enzymol.* **1987**, *81*, 333.
5. Shichida, Y.; Ono, T.; Yoshizawa, T.; Matsumoto, H.; Asato, A. E.; Zingoni, J. P.; Liu, R. S. H. *Biochemistry* **1987**, *26*, 4422.
6. Liu, R. S. H.; Crescitelli, F.; Denny, M.; Matsumoto, H.; Asato, A. E. *Biochemistry* **1986**, *25*, 7026.
7. Emsley, J. W.; Phillips, L.; Wray, V. *Prog. Nucl. Magn. Reson. Spectrosc.* **1997**, *10*, 85.
8. Colmenares, L. U.; Zou, X.-L.; Liu, J.; Asato, A. E.; Liu, R. S. H. *J. Am. Chem. Soc.* **1999**, *121*, 5803.
9. Wald, G. *Science* **1968**, *162*, 232.
10. Hellingwerf, J. *Photochem. Photobiol. B: Biol.* **2000**, *54*, 94.
11. Tierno, M. E.; Mead, D.; Asato, A. E.; Liu, R. S. H.; Sekiya, N.; Yoshihara, K.; Chang, C.-W.; Nakanishi, K.; Govindjee, R.; Ebrey, T. G. *Biochemistry* **1990**, *29*, 5948.
12. (a) Asato, A. E.; Li, X.-Y.; Mead, D.; Patterson, G. M. L.; Liu, R. S. H. *J. Am. Chem. Soc.* **1990**, *112*, 7398. (b) Liu, R. S. H.; Krogh, E.; Li, X.-Y.; Mead, D.; Colmenares, L. U.; Thiel, J. R.; Wong, D.; Asato, A. E. *Photochem. Photobiol.* **1993**, *58*, 701.

13. Muthyala, R.; Watanabe, D.; Asato, A. E.; Liu, R. S. H. *Photochem. Photobiol.*, in press.
14. Sheves, M.; Albeck, A.; Friedman, N.; Ottolenghi, M. *Proc. Natl. Acad. Sci. USA* **1986**, *83*, 3262.
15. (a) Tetreault, N.; Muthyala, R.; Liu, R. S. H.; Steer, R. J. *Phys. Chem.* **1999**, *103*, 2524. (b) Liu, R. S. H.; Muthyala, R.; Wang, X.-S.; Asato, A. E.; Wang, P.; Ye, C. *Org. Lett.* **2000**, *2*, 269-172.
16. (a) Kropf, A.; Whittenberger, B. P.; Goff, S. P.; Waggoner, A. S. *Exp. Eye Res.* **1973**, *17*, 591. (b) Lou, J.; Hashimoto, M.; Berova, N.; Nakanishi, K. *Organic Lett.* **1999**, *1*, 51, also *Methods Enzymol.* **2000**, *315*, 219.
17. (a) Kakitani, H.; Kakitani, T.; Yomosa, S. J. *Phys. Soc. Japan* **1997**, *42*, 996. (b) Han, M.; Smith, S. O. *Biochemistry* **1997**, *36*, 7280. (c) Tan, Q.; Lou, J.; Borhan, B., Karnaukhova, E.; Berova, N.; Nakanishi, K. *Angew. Chem. Int. Ed. Engl.* **1997**, *36*, 2089.
18. (a) Ito, M.; Hiroshima, T.; Tsukida, K.; Shichida, Y.; Yoshizawa, T. *J. Chem. Soc. Chem. Commun.* **1985**, 1443. (b) Katsuta, Y.; Sakai, M.; Ito, M. *J. Chem. Soc. Perkin Trans. I* **1993**, 2185.
19. Brewster, J. H. *J. Am. Chem. Soc.* **1959**, *81*, 5475.
20. (a) Barnes, C.; Djerassi, C. *J. Am. Chem. Soc.* **1962**, *84*, 1962. (b) Djerassi, C.; Osiecki, J.; Riniker, R.; Riniker, B. *J. Am. Chem. Soc.* **1958**, *80*, 1216. (c) Djerassi, C. *Optical Rotatory Dispersion*; McGraw-Hill: New York, 1960; pp 120-131.

About the Authors

Leticia U. Colmenares is currently an instructor at the Windward Community College, Hawaii, and associate researcher of the University of Hawaii (Manoa). She received her Ph.D. from the University of Hawaii (Manoa) in 1991. Her address is Department of Chemistry, University of Hawaii, 2545 The Mall, Honolulu, HI 96822.

Alfred E. Asato obtained his Ph.D. at the University of Hawaii at Manoa in 1972. He has remained on this campus as a postdoctoral researcher, assistant researcher and now an associate researcher.

Robert S. H. Liu obtained his Ph.D. at California Institute of Technology in 1965. After four years at DuPont, he moved to the University of Hawaii in 1968. Since 1972, he has been a professor of chemistry there. He considers the joint authorship between him and his mentor George S. Hammond spanning four decades (a recent one: Liu, R. S. H.; Hammond, G. S. *PNAS USA* **2000**, *97*, 11153) a major achievement of his. Since the beginning of this century, he has begun to test the water to become a free-lance photochemist in the Pacific region.

Copyright 2001 by the Center for Photochemical Sciences
The Spectrum is a quarterly publication of the Center for
Photochemical Sciences, Bowling Green State University,
Bowling Green, OH 43403.
Phone 419-372-2033 Fax 419-372-0366
Email photochemical@listproc.bgsu.edu
WWW <http://www.bgsu.edu/departments/photochem/>

Executive Director: D. C. Neckers
Principal Faculty: P. Anzenbacher, G. S. Bullerjahn,
J. R. Cable, F. N. Castellano,
M. E. Geusz, D. C. Neckers,
M. Y. Ogawa, V. V. Popik,
M. A. J. Rodgers, D. L. Snavely,
B. R. Ullrich
The Spectrum Editor: Pat Green
Production Editor: Alita Frater

COPYRIGHT PERMISSION

A person may make a single copy of any or all articles in this issue for personal use. Copying beyond that permitted by the U.S. Copyright law is allowed provided that the appropriate per copy fee is paid through the Copyright Clearance Center, Inc., 27 Congress St., Salem, MA 01970. For reprint permission, please write to the Center for Photochemical Sciences.

EDITORIAL POLICY

The Spectrum reserves the right to review and edit all submissions. *The Spectrum* is not responsible for contents of articles.

Articles submitted to *The Spectrum* will appear at the discretion of the editorial staff as space is available.

Multiphoton Microscopy and Its Applications in the Biomedical Sciences

Ammasi Periasamy, Colten Noakes, Masilamani Elangovan, Raymond Keller and Richard N. Day
University of Virginia

Introduction

Advances in optics, computers, digitizers, image processing, and low light level photodetectors have led to great improvements being made in fluorescence light microscopy technology.¹⁻⁴ Developments in fluorescent dyes that display the chemical and molecular dynamics of intact cells have significantly broadened the usage and applications of optical microscopy. These developments allow real-time observation and measurement of the activities of dye-marked constituents in cells and tissues. All light microscopy techniques can be used to view these dye-marked constituents and processes. However, digitized wide-field microscopy imaging contains out-of-focus information, which reduces the ability to view high-resolution images deeper inside the living specimen. The emission collected by a high numerical aperture objective lens comes from light excitation throughout the specimen, whether it is above or below the focal plane. This background autofluorescence seriously degrades the image by reducing its contrast and sharpness—it becomes impossible to determine true signal at the focal plane from background fluorescence from other focal planes. Two-photon microscopy has many more advantages for cellular imaging than one-photon excitation fluorescence microscopy.⁵⁻⁹ In multiphoton imaging, the photobleaching and autofluorescence are considerably reduced. Moreover, the number of photons reaching the detector is very high, since there is no pinhole used in front of the detector. The two-photon technique can be applied to a variety of biomedical applications where increased resolution and depth penetration into tissue are essential to studying marked processes. In this paper we discuss the basics and many biomedical applications of multiphoton microscopy.

Multiphoton Microscopy

Two-photon absorption was theoretically predicted by Goeppert-Mayer⁶ in 1931 and was experimentally observed for the first time in 1961 using a ruby laser as the light source.⁷ Denk and others has experimentally demonstrated two-photon imaging in a laser scanning confocal microscopy.⁵

In one-photon (wide-field or confocal) fluorescence microscopy, the absorption of laser energy excites the fluorescent molecules to a higher energy level and results in the emission of one photon of fluorescence. The fluorescence

intensity increases at a linear rate with the excitation intensity. Typically, some of the absorbed light energy is dissipated as heat, so the emission wavelength is longer than the absorption wavelength. For example, a fluorophore might absorb one-photon at 365 nm and fluoresce at a blue wavelength around 420 nm. Two-photon (2P) excitation occurs when two photons of $h\omega$ and $h\omega'$ are absorbed simultaneously and a molecule is excited to the state of energy $E = h\omega + h\omega'$. The probability that two-photon absorption will occur depends on the colocalization of two photons within the absorption cross section of the fluorophore.⁸ The rate of excitation is proportional to the square of the instantaneous intensity. This extremely high local instantaneous intensity is produced by the combination of diffraction-limited focusing of a single laser beam in the specimen plane and the temporal concentration of a femtosecond (fsec) mode-locked laser³ (typically of the order of 10^{-50} to 10^{-49} cm⁴ s / photon / molecule).

The fluorophores exhibit two-photon absorption at approximately twice (680 nm) their one-photon absorption wavelengths, while two-photon emission is the same as that of one-photon (420 nm), allowing the specimen to be imaged in the visible spectrum. When an infrared

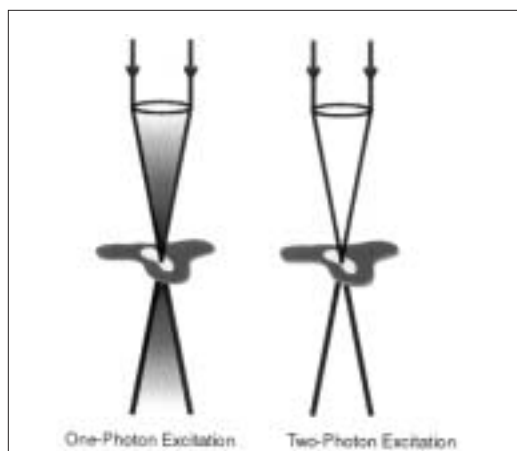


Figure 1. Illustration of the excitation light paths for wide-field or confocal microscopy and two-photon (2p) excitation fluorescence microscopy.

laser beam is focused on a specimen, it illuminates at a single point and the fluorescence emission is localized to the vicinity of the focal point. The fluorescence intensity then falls off rapidly in the lateral and axial direction. In one-photon microscopy, illumination occurs throughout the excitation beam path (as shown in Figure 1), in an hourglass-shaped path. This results in absorption along the excitation beam path, giving rise to substantial fluorescence emission both below and above the focal plane. Excitation from other focal planes contributes to photobleaching and photodamage in the specimen planes that are not being involved in imaging. The infrared illumination in two-photon excitation also penetrates deeper into the specimen than visible light excitation due to its higher energy, making it ideal for many applications involving depth penetration through thick sections of tissue.

The three-photon absorption is a natural extension of two-photon absorption and arises from third-order perturbation treatment. At least two intermediate states are required for the transition, and so, many resonance conditions occur. Even though it is difficult to compare the cross sections for two- and three-photon excitation, the emission intensities resulting from three-photon excitation are large and comparable to within a factor of ten to those of two-photon excitation. Further possible advantages of three-photon excitation include the higher polarization and wavelength-dependent photoselection and the availability of 800-1000nm fs pulses from solid state ti:sapphire lasers.

Instrumentation

The Multiphoton microscopy system⁹ consists of a Nikon TE300 epifluorescent microscope with a 100W Hg Arc Lamp for transillumination. A PlanFluor 20x, NA 0.75 multiimmersion (water and oil) objective lens was used for the image acquisition. A built-in lens and the dichroic in the filter cube were used to couple the TE300 externally (no physical connection between microscope and the confocal scan head) to the confocal laser head. A Coherent 5W Verdi pumped, tunable (model 900 Mira) modelocked ultrafast (76MHz) pulsed laser (Coherent Inc., Santa Clara, CA) was coupled to the laser port of a BioRad MRC600 (BioRad, Hercules, CA) laser scanning confocal scan head through beam steering optics. This laser was equipped with x-wave optics for easy tunable range of the entire wavelength (720 to 920 nm). The silver-coated mirrors for maximum reflections of IR and visible spectrum (Chroma Technology Corp.) replaced the MRC600 conventional mirrors M1, X- and Y- galvo, and concave (1 and 2) mirrors. The controller card of the MRC600 and the DOS-based software COMOS 7.0a were installed in a 450 MHz Pentium operating Windows '98. Confocal Imaging Assistant was used to convert the BioRad PIC file into separate TIF files for analysis.

Applications

Developmental Biology

The two-photon excitation (TPEM) approach has two significant advantages over other methodologies for developmental biology: (1) it can see deeper and clearer into tissue than either deconvolution (DDM) or confocal microscopy (LSCM), and (2) it has the advantage of causing considerably less photodamage than the non-confocal excitation fluorescence techniques. To be a useful method for studying frog morphogenesis several additional criteria must be met. First, the technique must be compatible with living frog tissue over a period of hours, at framing rates of 12-20/hour and with more z-series information collected. Second, imaging of the active cells must be possible in the tissues undergoing morphogenesis, and these can be buried in the tissue. Currently, the two-photon is the only tested fluorescence microscopy technique that meets these minimum requirements.⁹ The images were collected in developing Xenopus embryo to localize the GFP-GAP-43 fusion proteins using TPEM, LSCM, and DDM as explained in the literature.⁹ The objective lens (PlanFluor 20x, NA 0.75 multiimmersion lens) used for the data collection is the same as what we used for the TPEM images. The deconvolution processing was also implemented as explained in the literature⁹ for the GFP-GAP-43 fusion proteins (see Figure 2).

Multiphoton Fluorescence Resonance Energy Transfer Microscopy (MP-FRET)

In the late 1940s Förster proposed the theory of FRET, which described how energy could be transferred directly from a fluorophore in the excited state (the donor, D) to a non-identical acceptor (A) fluorophore.¹⁰⁻¹² The transfer of excited state energy occurs without the production of heat and does not require that a collision occur between D and A.

The energy from D can be transferred directly to A under the following four conditions: (i) when the emission spectrum of the donor overlaps the absorption spectrum of the acceptor by a considerable percentage; (ii) when the two fluorophores are within ~1 to ~10 nm of each other; (iii) when the donor emission dipole moment, the acceptor absorption dipole moment, and their separation vectors are in favorable mutual orientation; and (iv) when the emission of the donor has a reasonably high quantum yield.

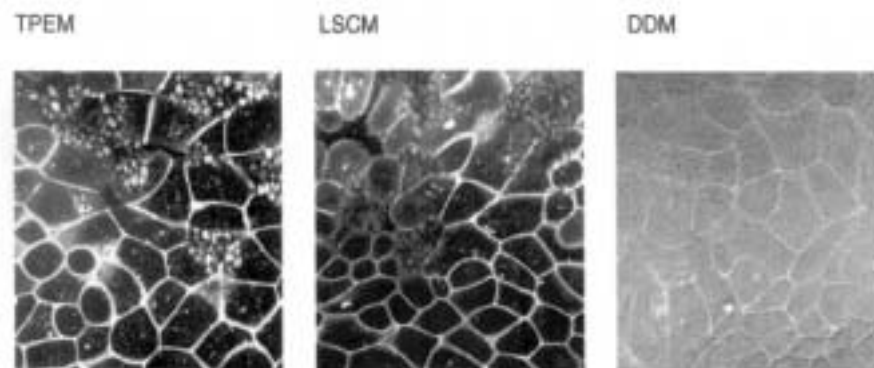


Figure 2. Localization of GFP-GAP-43 fusion protein images in developing *Xenopus* embryos were acquired with same objective lens using Nikon epi-fluorescence based two-photon excitation microscopy (TPEM), laser scanning confocal microscopy (LSCM), and wide-field microscopy using digital deconvolution (DDM). The details of the images are superior in TPEM. Generally, deterioration and less details of information of GFP-GAP-43 proteins were observed in all sections of the tissue in LSCM mode. The DDM system is not good for tissue imaging as demonstrated in the figure (images were deconvolved with 15 iterations using the Deltavision software).

Conventional or different mutant forms of green fluorescent proteins (GFP) could be used as fluorophore pairs.¹³⁻¹⁶ It is important to note that one should have a good expression (or labeling) level of proteins with the selected fluorophore. It is also important to use better optics and high quantum efficiency detectors to acquire the FRET images. One of the fluorophores spectral emission (donor) should have at least a 30% overlap with the absorption spectrum of the other (acceptor) fluorophore.

Pituitary GHFT1-5 cells¹⁵ expressing the RFP (DsRed) tagged C/EBP α protein were identified by 543 nm excitation using an arc lamp light source coupled to the 2p-FRET microscope. We selected appropriate filters and high sensitivity PMTs to acquire D and A images. The emission filters for donor (460/40 nm) and acceptor (610/60 nm) were assembled in a filter cube with an appropriate dichroic mirror (500 nm, long pass) (www.chroma.com). This filter cube was positioned and aligned in the Biorad MRC600 scan head for maximum signal to the respective PMTs or channels. For 2p excitation, the ti:sapphire laser wavelength was tuned from 900 nm down to 700 nm in order to see minimum or no signal from the RFP-C/EBP α alone labeled proteins (acceptor). For 870 nm excitation wavelength we found no or less RFP signal in the acceptor channel. The CFP-C/EBP Δ 244 protein molecule (donor) was excited with 870 nm wavelengths from the ti:sapphire laser, which caused a considerable amount of signal in the donor channel. This infrared wavelength excitation of CFP fluorophore considerably reduces the photobleaching compared with 365 nm UV light excitation in conventional fluorescence microscopy. The 870 nm was used as an excitation wavelength to acquire the donor and acceptor images from doubly expressed cells (CFP-RFP-C/EBP Δ 244). One could visualize both the donor (D) and acceptor (A) images in a single slow scan mode. The image "A" is a contaminated FRET image and that should be corrected before calculating the distance between D and A.

Each fluorophore molecule used for FRET imaging has a characteristic absorption and emission spectrum that should be considered for characterizing the FRET signal acquired using these microscopic techniques. Moreover, there are other problems encountered in FRET microscopy imaging such as autofluorescence, detector and optical noise, photobleaching, and spectral bleed-through signal.¹⁴ In addition to these noises one should also consider the expression level or fluorophore concentration of each cell used for FRET imaging. It is important to implement the correction in order to quantitate the FRET signal or in calculating the distance between two proteins. We developed a software package that will provide many options to correct the above-mentioned noises in the acceptor image to obtain a true FRET image (see Figure 3).

Multiphoton Fluorescence Lifetime Imaging Microscopy (MP-FLIM)

An important advantage of these time-resolved fluorescent lifetime measurements is that they are independent of probe concentration, and other factors that limit intensity-based steady-state measurements. Moreover, competing

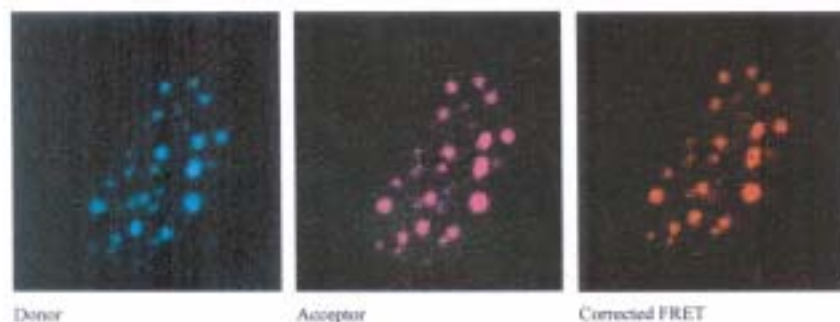


Figure 3. Localization of CFP- and RFP-C/EBP Δ 244 protein expressed in GHFT1-5 cells using 2p-FRET microscopy. The doubly expressed cells (CFP-RFP-C/EBP Δ 244) were excited by 870 nm and the donor and acceptor images of proteins localized in the nucleus of a single living cell were acquired by single scan (slow scan). As explained in the text, the bleed-through (or cross talk) correction was implemented to obtain a FRET image (Corrected FRET). (Donor-Cyan color, Uncorrected FRET-pink color, and Corrected FRET-red color dots)

environmental and competing physical processes, such as resonance energy transfer and quenching, can alter the fluorescence lifetime; thus, measurements of fluorescence lifetimes can provide a very accurate reflection of the probe's local environment. The FLIM system will not only be used for FRET but also for various biological applications from single cells to single molecules for the tissue culture cell as well as deep tissue cellular imaging.

The fluorescence lifetime is the average time that a molecule remains in an excited state prior to returning to the ground state. For single exponential decay of fluorescence, the fluorescence intensity as a function of time after a brief pulse of excitation light is described as¹²

$$I(t) = I_0 \exp(-t/\tau) \quad [1]$$

where I_0 is the initial intensity immediately after the excitation pulse. Thus, the time in which the fluorescence intensity decays to $1/e$ of the intensity immediately following excitation is the lifetime (τ). In practice, fluorescence decay is often multiexponential, leading to complex decay curves.

The average time that a fluorophore spends in an excited state is typically less than 100 nanoseconds, and the duration of the excited state, i.e., its fluorescence lifetime, is critically dependent upon the local environment surrounding the probe. Because biological interactions occur over a similar time-scale, monitoring the localized changes in probe fluorescence lifetime provides an enormous advantage for imaging dynamic cellular events.¹⁷ For example, proteins labeled with fluorophores may exist in environmentally distinct regions of a cell that all have similar fluorescence intensity distribution, but may exhibit regional differences in the fluorescence lifetimes for the probe. The measurement of fluorescence intensity alone would not indicate these differences, but imaging of the fluorescence lifetime could reveal these different sub cellular environments.

The Becker & Hickl GmbH (<http://www.becker-hickl.de>) company has developed a system called a photon-counting module (TCSPC, SPC-730), which could be coupled to any scanning microscope. The signal from the photomultiplier tube (PMT) should be synchronized with the scan control signals (pixel clock, Line sync, Frame sync) from the respective scan control unit. Synchronization with the laser pulse sequence is achieved by the SYNC signal from the reference laser pulse. The time resolution depends on the detector. The PMT detector has a time resolution of 25 ps. For each PMT pulse, i.e. for each photon, the TCSPC module determines the time of the photon within the laser pulse sequence and the location within the scanning area. These values are used to address the histogram memory in which the events are accumulated. Thus, in the memory the distribution of the photon density over x , y , and the time within

the fluorescence decay function builds up. The result can be interpreted as a two-dimensional (x, y) or three-dimensional (x, y, t) array of fluorescence decay curves or as a sequence of fluorescence images for different times after the excitation pulse. Due to the short dead time of the SPC-730 module nearly all detected photons are processed and accumulated in the histogram for further calculation and display. Using the SPC-730 TCSPC lifetime imaging module one could achieve lifetime images at different focal plane or at different location of the cell or tissue. The FLIM images should be accumulated for a few minutes to obtain a better signal to noise ratio (S/N).

As mentioned in the MP-FRET section the intensity based or steady state FRET imaging does introduce errors in calculating the distance between the donor and acceptor molecules. Moreover, the spectral bleed-through, or cross talk, is a problem to recognize whether one is observing the sensitized emission or the bleed-through signals. Also, the strength of the signal depends on the excitation intensity and the fluorophore concentration. In contrast, FLIM or lifetime measurements are independent of excitation intensity or fluorophore concentration. The combination of FLIM and FRET will provide high spatial (nanometer) and temporal (nanoseconds) resolution when compared to steady state FRET imaging. Importantly, spectral bleed-through is not an issue in FLIM-FRET imaging because only the donor fluorophore lifetime is measured.¹⁸ The presence of acceptor molecules within the local environment of the donor that permit energy transfer will influence the fluorescence lifetime of the donor. By measuring the donor lifetime in the presence and the absence of acceptor one can accurately calculate the distance between the donor- and acceptor-labeled proteins.¹⁸

Multiphoton Fluorescence Correlation Spectroscopy (MP-FCS)

Fluorescence correlation spectroscopy (FCS) is a technique in which temporal fluctuations in the fluorescence measured from a sample of fluorescence molecules are analyzed to obtain information about the processes that give rise to the fluorescence fluctuations. The temporal autocorrelation of the fluorescence fluctuations, which measures the average duration of a fluorescence fluctuation, decays with time. The rate and shape of the decay of the autocorrelation function provide information about the mechanisms and rates of the processes that generate the fluorescence fluctuations. The magnitude of the autocorrelation function provides information about the number densities of fluorescent species in the sample region.

The image correlation spectroscopy is the imaging analog of temporal FCS. These methods are characterized by the spatial autocorrelation analysis of fluctuations in fluorescence intensity arising from a microscopic illumination volume defined by the diffraction limited focus of the excitation laser beam. The fluorescence fluctuation record inherently contains information about both the absolute concentrations of the fluorescent molecules and their state of aggregation as well as the dynamic properties of these molecules. Low noise (<300 counts/sec) avalanche photodiodes (APD; SPCm-AQR-16-FC, EG & G, Vaudreuil, Quebec, Canada) of active area of about 0.8mm could be coupled to the microscope for single and dual color two-photon fluorescence correlation spectroscopy. The output of the photon counting detectors will be sent directly to an ALV-6000 correlator (ALV GMBH, Langen, Germany) where auto- and cross-correlation functions would be calculated. The correlators should be synchronized with the system for image correlation spectroscopy.

The time range in which FCS has been the most successful is between 10 μ s and 100 μ s, and FCS is thus complementary to faster techniques such as FLIM anisotropy and to slower techniques such as fluorescence photobleaching recovery. There are large number of parameters that could be measured with FCS including translational diffusion coefficients, chemical kinetic rate constants, rotational diffusion coefficients, flow rates, molecular weights, and molecular aggregation. Measurement of these physical parameters has been used for a range of purposes, including an increased understanding of protein, nucleic acid, and lipid diffusion, solution and interfacial kinetics, cell surface receptor and macromolecular clustering, and the detection of antibodies and viruses. It has been demonstrated that the diffusion coefficients on the order of 10^{-8} to 10^{-12} cm^2/s could be measured using the MP-FCS system and that would cover the complete range of transport phenomena within the cellular membrane.¹⁹

As an example the temporal two-photon image correlation spectroscopy studies of the α_5 integrin-GFP constructs on living CHO fibroblasts at 37 °C are beginning to provide spatial maps of molecular dynamics in different regions of the basal membrane. Additionally, they were able to measure aggregation events as they occur in time using this cell system and two-photon image correlation measurements (Ex-890 nm; BioRad RTS-2000). From the data analyzed thus far, it has been observed that diffuse integrins at the leading edge are immobilized and that there is robust transport of integrins throughout the cell.²⁰

Conclusion

In this paper we described the basics and integration of a multiphoton microscope using the Biorad MRC600 laser scanning confocal microscope. The comparison of two-photon, LSCM, and DDM clearly demonstrate that one would prefer to use multiphoton microscopy for developmental biological applications. We also demonstrated that the MP-FRET technique is a viable technique to localize the protein in a single living cell nucleus. We described another two multiphoton techniques (MP-FLIM, MP-FCS), which could be used to study the protein dynamics in living specimens.

Acknowledgments

This work was supported by grants from the W. M. Keck Foundation.

References

1. Bright, G. R.; Taylor, D. L. In *Applications of Fluorescence in the Biomedical Sciences*; Alan R. Liss: New York, 1986; p 257.
2. Inoué, S.; Spring, K. *Video Microscopy*, 2nd ed.; Plenum Press: New York, 1997.
3. Pawley, J. *Handbook of Biological Confocal Microscopy*, 2nd ed.; Plenum Press: New York, 1995.
4. *Methods in Cellular Imaging*; Periasamy, A., Ed.; Oxford University Press: New York, 2001.
5. Denk, W.; Strickler, J. H.; Webb, W. W. *Science* **1990**, *248*, 73.
6. Goppert-Mayer, M. *Ann. Phys.* **1931**, *9*, 273.
7. Kaiser, W.; Garrett, C. G. B. *Phys. Rev. Lett.* **1961**, *7*, 229.
8. Xu, C.; Webb, W. W. *J. Opt. Soc. Am. B* **1996**, *13*, 481.
9. Periasamy, A.; Skoglund, P.; Noakes, C.; Keller, R. *Microsc. Res. & Tech.* **1999**, *47*, 172.
10. Förster, T. In *Modern Quantum Chemistry*; Academic Press: New York, 1965; pp 93-137.
11. Stryer, L. *Annu. Rev. Biochem.* **1978**, *47*, 819.
12. Lakowicz, J. R. *Principles of Fluorescence Spectroscopy*; Plenum Press: New York, 1986.
13. Heim, R.; Tsien, R. Y. *Curr. Biol.* **1996**, *6*, 178.
14. Periasamy, A.; Elangovan, M.; Wallrabe, H.; Demas, J. N.; Barroso, M.; Brautigan, D. L.; Day, R. N. In *Methods in Cellular Imaging*; Oxford University Press, 2001; Chapter 17.
15. Day, R. N.; Periasamy, A.; Schaufele, F. *Methods* **2001**, *25*, 4.
16. Periasamy, A.; Day, R. N. *Methods Cell Biol.* **1999**, *58*, 293.
17. Periasamy, A.; Wodnicki, P.; Wang, X. F.; Kwon, S.; Gordon, G. W.; Herman, B. *Rev. Sci. Instrum.* **1996**, *67*, 3722.
18. Elangovan, M.; Day, R. N.; Periasamy, A. *J. Microsc.* January 2002, in press.
19. Peterson, N. O.; Hoddellius, P. L.; Wiseman, P. W.; Seger, O.; Magnusson, K.-E. *Biophys. J.* **1993**, *65*, 1135.
20. Wiseman, P. W.; Squier, J. A. *SPIE* **2001**, *4262*, 279.

About the Authors

Dr. Ammasi Periasamy received his Ph.D. in Biomedical Engineering at the Indian Institute of Technology, Madras. He is currently a Professor of Biology and Biomedical Engineering and a Center Director for the Keck Center for Cellular Imaging (KCCI; www.cci.virginia.edu). His address is W. M. Keck Center for Cellular Imaging, University of Virginia, Department of Biology, Gilmer Hall (039), Charlottesville, Virginia 22904. Colten Noakes and Masilamani Elangovan are KCCI staff. Dr. Raymond Keller received his Ph.D. at the University of Illinois. He is currently Professor and Chair of the Department of Biology. Dr. Richard Day received his Ph.D. in Pharmacology at the University of Rochester. He is currently an Associate Professor of Medicine and Cell Biology.

Center for Photochemical Sciences Publications

415. Aoudia, M.; Guliaev, A. B.; Leontis, N. B.; **Rodgers, M. A. J.** Self-assembled complexes of oligopeptides and metalloporphyrins: measurements of the reorganization and electronic interaction energies for photoinduced electron transfer reactions. *Biophys. Chem.* **2000**, *83*, 121-140.
416. Zang, L.; **Rodgers, M. A. J.** Diffusion-controlled charge transfer from excited Ru(bpy)₃³⁺ into nonosized TiO₂ colloids stabilized with EDTA. *J. Phys. Chem. B* **2000**, *104* (3), 468-474.
417. Strehmel, B. Fluorescence probes for material science. In *Advanced Functional Molecules and Polymers*; Nalwa, H. S., Ed.; Gordon & Breach, 2000; Chapter 7, pp 287-370.
418. Sessler, J. L.; **Anzenbacher Jr., P.**; Shriver, J. A.; Jursíková, K.; Lynch, V. M.; Marquez, M. Direct synthesis of expanded fluorinated calix[n]pyrroles: decafluorocalix[5]pyrrole and hexadecafluorocalix[8]pyrrole. *J. Am. Chem. Soc.* **2000**, *122* (48), 12061-12062.
419. Jarikov, V. V.; **Neckers, D. C.** Anionic photopolymerization of methyl 2-cyanoacrylate and simultaneous color formation. *Macromolecules* **2000**, *33*, 7761-7764.
420. **Ullrich, B.** Absorption dichroism of thin CdS films formed by pulsed-laser deposition. Presented at Symposium on Compound Semiconductors, Monterey, CA, 2000.
421. Jarikov, V. V.; **Neckers, D. C.** Photochemistry of triarylmethane dye leuconitriles. In *Advances in Photochemistry*; Wiley & Sons: New York, 2001.
422. Gu, H.; Ren, K.; Grinevich, O.; Malpert, J.; **Neckers, D. C.** Characterization of iodonium salts differing in the anion. *J. Org. Chem.* **2001**, *66* (12), 4161-4164.
423. Zhou, X.; Tyson, D. S.; **Castellano, F. N.** First generation light-harvesting dendrimers with a [Ru(bpy)₃]²⁺ core and aryl ether ligands functionalized with coumarin 450. *Angew. Chem. Int. Ed.* **2000**, *39* (23), 4301-4305.
424. Ranatunga, A.; Lasey, R. C.; **Ogawa, M. Y.** The localization of hydrophilic sites within an osmium polypyridyl compound can produce a negative activation energy for emission decay. *Inorg. Chem. Commun.* **2000**, *4* (1), 30-32.
425. Li, H.; Ren, K.; Zhang, W.; Malpert, J. H.; **Neckers, D. C.** A novel initiation system for the cationic polymerization of glycidyl phenyl ether: triphenylcyclopropenium tetrakis(pentafluorophenyl)gallate / cyclohexanone. *Macromolecules* **2001**, *34*, 2019.
426. Sen, A.; Dwivedi, S.; Rice, K. A.; **Bullerjahn, G. S.** Growth phase and metal-dependent regulation of the *dpsA* gene in *Synechococcus* sp. stain PCC7942. *Arch. Microbiol.* **2000**, *173*, 451-456.
427. Hoostal, M.; **Bullerjahn, G. S.**; McKay, R. M. L. Development of a PCR-based assay for PCB bioremediation in aquatic sediments. *Hydrobiologia* **2001**, in press.
428. Jarikov, V. V.; **Neckers, D. C.** Photochemistry and photophysics of triarylmethane dye leuconitriles. *J. Org. Chem.* **2001**, *66*, 659-671.
429. Fedorov, A. V.; Danilov, E. O.; **Rodgers, M.A.J.**; **Neckers, D. C.** Time-resolved step-scan fourier transform infrared spectroscopy of alkyl phenylglyoxylates. *J. Am. Chem. Soc.* **2001**, *123*, 5136-5137.
430. Kaafarani, B. R.; **Neckers, D.C.** Photocyclization of a conjugated triaryl 'Y-enyne'. *Tetrahedron Lett.* **2001**, *42*, 4099-4102.

For reprints of any of these publications, please write or e-mail the Center for Photochemical Sciences and refer to the reprint by number. Reprints of articles in press will be provided upon publication of the article.

If "1,000 scans per second" sounds too esoteric for you, recall how recently people wondered what to do with computers.

Highest speed, submilliabsorbance sensitivity, easy modularity, fully digital operation, and real-time global fitting software are not esoteric, but are the result of bringing together today's best technologies on one optical bench.



DeSa Monochromator

Based on Dr. Richard DeSa's patented double monochromator, the Olis RSM 1000 spectrometers are ideal for fast reaction kinetic studies, such as stopped-flow and flash/photolysis. Other applications are regular spectral scanning, dual wavelength, and fixed wavelength detection.

One Olis RSM 1000 can be your best time-resolved spectrophotometer. And your best time-resolved spectrofluorimeter. And your best time-resolved circular dichroism spectrometer. And a routine scanning spectrometer for all those daily measurements your group must make. In other words, *1,000 scans per second is just the beginning!*



Contact Olis for all the details: 800-852-3504 □ 706-353-6547 (worldwide) □ olis@negia.net □ www.olisweb.com

Your ad on this page will reach 7,000 scientists
in 50 countries worldwide.

Contact pvgreen@earthlink.net